

THEORY AND MEASUREMENTS OF LABYRINTH SEAL COEFFICIENTS FOR
 ROTOR STABILITY OF TURBOCOMPRESSORS

H.R. Wyssmann
 Sulzer-Escher Wyss Ltd
 Zurich, Switzerland

The prediction of rotordynamic coefficients for gas seals is achieved with the aid of a two-volume bulk flow model based on turbulent rotationally symmetric 3D flow calculations including swirl flow. Comparison of cross-coupling and damping coefficients with measurements confirm this approach. In particular the theoretically predicted phenomenon that labyrinth damping is retained without inlet swirl is confirmed. This is important for the design of high pressure compressors, where labyrinth damping is a major contribution improving rotor stability. Discrepancies are found when comparing theory with measured direct stiffness and the cross-coupling damping coefficients. First measurements of labyrinth seals on a recently installed test rig operated with water are presented. Since forces are larger than on test stands operated with air and since individual chamber forces are obtained phenomena like inlet effects may be studied.

INTRODUCTION

For many years radial seal forces have been studied and investigated for stability of turbomachinery, especially for pumps and turbocompressors. Many papers on this subject have appeared, most of them either presenting measurements or a theoretical approach. Few authors have compared measurements with theory, mainly because a reasonably simple theory producing results in reasonable agreement with measurements was not available. The author in a former paper has presented a theory based on a two volume bulk flow approach, incorporating results from 3D finite difference calculation of the rotationally symmetric single cavity turbulent flow, based on time averaged Navier Stokes equations with a k- ϵ turbulence closure. Comparison of the results for cross-coupling coefficients of straight through labyrinths with measurements showed good agreement. However, test results were not available at the time for labyrinth damping, which the theory predicted to be substantial compared to bearing damping at high densities found in turbocompressors for the oil and gas industry. This paper attempts to present the latest findings both on the theoretical side and in measurements for the straight through seal with teeth on stator or on rotor. For the larger part the measurements have been carried out at the Turbomachinery Laboratories at Texas A&M University.

SYMBOLS

a	area of cross-section between 2 strips	e	eccentricity
A	area of cross-section of labyrinth channel	h	labyrinth strip height
b_Q	cross-coupling damping	k_Q	cross-coupling stiffness
b_R	direct damping	k_R	direct stiffness
c_f	friction coefficient	l	mixing length
d	distance between two strips	\dot{m}	leakage flow rate through labyrinth

\dot{m}_r	mass rate exchange between 2 control volumes	ν	viscosity
p	pressure	ρ	density
Q	cross-coupling force	τ	stress
R	direct force	φ	angle
r	labyrinth radius	Subscripts:	
Δr	radial clearance of concentric labyrinth	in	inlet
t	time	j	jet
w	circumferential velocity	r	rotor or radial
z	number of labyrinth strips	s	stator
β	mixing factor	out	outlet
δ	radial clearance of eccentric labyrinth		
μ	labyrinth flow coefficient		

THEORY

The theory gives the solution for the circumferential pressure distribution of straight through labyrinths for gas and (incompressible) hydraulic flow. With some modifications, the theory is also applicable for staggered and full labyrinths. Here only a summary of the theory is given. More detailed results may be found in [10]. The calculation is based on bulk flow assumptions, i.e. on a uniform flow profile in the region between the strips and (a different) uniform profile between strip tips and bushing (for rotor seal) or rotor (for stator seal). This is schematically depicted in Fig. 1. The validity of the assumed velocity profiles has been confirmed by extensive numeric flow calculations for the rotationally symmetric 3D turbulent flow in a single chamber. In these the velocity field v is decomposed into a time averaged part \bar{v} and a turbulent fluctuation part v' :

$$v = \bar{v} + v'. \quad (1)$$

The continuity equation for v , assuming incompressibility within the chamber, reads after insertion of (1) and time averaging:

$$\nabla \cdot \bar{v} = 0.$$

where ∇ denotes the Nabla Operator.

The time averaged Navier Stokes equations become:

$$\partial \bar{v} / \partial t + (\bar{v} \cdot \nabla) \bar{v} = - \nabla p + \nabla \nu \times \nabla \times \bar{v} + \text{turbulent diffusion}.$$

The turbulent diffusion term is described by a two parameter model, based on $k = 1/2 v_i' v_i'$, the turbulent kinetic energy and $\epsilon = \nu \partial v_i' / \partial x_j \partial v_j' / \partial x_i$, the dissipation rate of the kinetic fluctuation energy. For k and ϵ transport equations may be written down with a total of 5 empiric parameters. Correlation of the parameters to flow measurements has been given by Stoff [8].

As boundary conditions, the pressure difference across the chamber, the rotational speed and the inlet circumferential velocity are given. The numerical calculations yield the pressure and velocity distributions (time averaged) within the chamber. The analysis does not consider the flow contraction across the strip however. The results of this analysis has been used for the modelling of the eccentric quasi-stationary flow in the labyrinth chamber as given below. The following equations are valid for seals with strips on the

rotor, similar equations hold for stator seals. The field equations for the two control volumes in Fig. 1 read:

$$\text{Continuity:} \quad a\partial w_i/\partial\phi + \delta d\delta w_m/\partial\phi - w_m d\delta/\partial\phi - r\partial A/\partial t = 0, \quad (2)$$

$$a\partial w_i/\partial\phi - \dot{m}_r/\rho = 0. \quad (3)$$

$$\text{Momentum:} \quad \begin{aligned} & -2\rho a w_i \partial w_i/\partial\phi - 2\rho \delta d w_m \partial w_m/\partial\phi - \rho w_m^2 d\delta/\partial\phi + \\ & \quad + \dot{m}(w_{in} - w_{out}) - a_r r \tau_r - \\ & - a_s r \tau_s - \rho r d(\delta w_m)/\partial t - \rho r a \partial w_i/\partial t = A \partial p/\partial\phi \end{aligned} \quad (4)$$

$$\begin{aligned} & -2\rho a w_i \partial w_i/\partial\phi + \dot{m}_r w_o - a_r r \tau_r - \\ & - d r \tau_j - \rho r a \partial w_i/\partial t = a \partial p/\partial\phi. \end{aligned} \quad (5)$$

Here, the w 's denote the circumferential velocity components of the flow: w_i the velocity of the core flow between the strips, w_m of the free jet between strip tips and stator and w_o the circumferential velocity at the interface between the two flow regions.

The axial flow is described by the classical leakage equation for the compressible flow through a seal (see Neumann [6], for instance):

$$\dot{m} = 2\pi\mu r \delta \rho_o \sqrt{(p_o/\rho_o)} \sqrt{(1 - \pi_p^2)/z}. \quad (6)$$

The flow coefficient μ follows the definition of Neumann [6] and takes into account the labyrinth strip geometry.

The turbulent wall shear stresses are given by

$$\text{for the rotor, and} \quad \tau_r = 1/2 c_{fr} \rho |w_i - w_{rot}| (w_i - w_{rot}) \quad (7)$$

$$\tau_s = 1/2 c_{fs} \rho \sqrt{(c_{ax}^2 + w_m^2)} w_m \quad (8)$$

for the stator, where the friction coefficients c_{fr} and c_{fs} are calculated with Prandtl's universal law for the tube flow.

The interaction of the two flow regions is described by a turbulent free shear stress τ_j modelled according to Prandtl's mixing length theory:

$$\tau_j = \rho l^2 |\partial u/\partial y| |\partial u/\partial y|,$$

where u is the flow velocity in the shear flow zone. For free jets, an obvious choice for the mixing length l is the mixing thickness b (Abramovich [1]). For the obstructed jet flow at hand, a proportionality factor β is introduced, such that $l = \beta b$, where β is a function of the labyrinth geometry. β has been determined by correlation of the (bulk flow) solution of the concentric labyrinth to the 3D finite difference calculations of the rotationally symmetric flow described above and to measurements.

In order to obtain the stiffness and damping coefficients of the seal, a first order solution of the equations (2) through (8) in e and \dot{e} is sufficient. Hence, the gap between strips and stator may be written as

$$\delta = \Delta r + e(t) \cos\phi,$$

where $e/\Delta r \ll 1$. The flow quantities and the pressure in equations (2) through (8) may therefore be written as:

$$\begin{aligned} w_i &= \bar{w}_i + \tilde{w}_i(\varphi, t), & m &= \bar{m} + \tilde{m}(\varphi, t), \\ w_m &= \bar{w}_m + \tilde{w}_m(\varphi, t), & p &= \bar{p} + \tilde{p}(\varphi, t). \end{aligned}$$

The zeroth order solution describes the concentric labyrinth and has been used to determine the mixing factor β by correlation to the 3D finite difference calculations of the rotationally symmetric flow described above.

The pressure $p(\varphi, t)$, linear in e and e is obtained upon integration of the linearization of equations (2) through (8). The force components acting on the rotor read:

$$Q = \int_0^{2\pi} \tilde{p} \sin \varphi r d\varphi, \quad R = \int_0^{2\pi} \tilde{p} \cos \varphi r d\varphi, \quad (9)$$

with Q orthogonal to and R in line (but opposite) with the rotor eccentricity e . In cartesian coordinates the force components may be written as:

$$\begin{bmatrix} K_x \\ K_y \end{bmatrix} = - \begin{bmatrix} k_R & k_Q \\ -k_Q & k_R \end{bmatrix} \begin{bmatrix} x \\ y \end{bmatrix} - \begin{bmatrix} b_R & b_Q \\ -b_Q & b_R \end{bmatrix} \begin{bmatrix} \dot{x} \\ \dot{y} \end{bmatrix} \quad (10)$$

where k_R = stiffness, k_Q = cross-coupling stiffness, b_R = damping, and b_Q = cross-coupling damping of the seal.

For staggered and straight labyrinths, a similar theory may be applied. 3D calculations of the concentric labyrinths have shown the circumferential velocity to be almost uniform across the whole chamber here, hence a single circumferential velocity may be assumed [10].

COMPARISON OF CROSS-COUPLING STIFFNESS WITH MEASUREMENTS

The cross-coupling coefficients obtained from the theory as presented above has been compared to measurements carried out by different authors. It agrees well with the laboratory measurements carried out by Benckert [2] for various types of labyrinths. The least agreement has been found for staggered and full labyrinths. For reference see [10]. Measurements on a real compressor at high pressures with Nitrogen have been carried out for the first time by the authors company. The circumferential pressure distribution of the first stage impeller shroud seal in a four stage natural gas compressor designed for a discharge pressure of 320 bar has been measured for different rotor eccentricities relative to the seal. Fig. 2 shows the test labyrinth in the lower half of the inner casing. The measurements have been carried out with and without a swirl brake (Fig. 3) to confirm the theoretically predicted influence of the inlet swirl velocity on cross-coupling stiffness. The circumferential velocity of the leakage flow was measured by pitot tubes in front of the first labyrinth strip and has been used as inlet condition for the calculation. Fig. 4 shows measured and calculated cross-coupling stiffness of the seal for different pressure levels and rotor speeds. The theory agrees well with measurements. With swirl brake installed, theory gives less negative cross-coupling than found by measurement. However, the absolute value of the cross-coupling stiffness compared to the case without swirl brake is very small (scale in Fig. 4 is blown up by factor 10 for case with swirl brake), hence for practical applications this discrepancy has no importance. All these tests could not produce damping coefficients, but they basically confirmed the theoretical approach presented above. They also confirmed the dominating influence of the inlet swirl velocity on the magnitude of the cross-coupling coefficients and hence were in line with the many cases where rotor stability problems have been solved by reducing the inlet swirl velocity of the labyrinth leakage flow. The theory however predicts damping coefficients of labyrinth seals of a magnitude to improve substantially the rotor damping for high pressure compressors. Hence, a confirmation by measurements is of great importance.

COMPARISON OF FULL SET OF LABYRINTH COEFFICIENTS WITH MEASUREMENTS

A test rig for air seals has been set up at the Turbomachinery Laboratories of Texas A&M University, capable to measure the full set of labyrinth coefficients as defined by (10). The rotor is moved by a hydraulic shaker performing translatory movements. By measuring the reaction forces the dynamic coefficients can be identified. This differs from the measurements described above, where forces were obtained by integration of pressures. Extensive measurements have been carried out with straight- through teeth on stator and teeth on rotor labyrinth seals with 16 chambers by Childs and Scharrer ([3], [7]). Rotor speed varied between 500 and 8000 RPM or 4 m/s to 63 m/s in circumferential velocity, inlet pressures between 3.08 and 8.25 bar (against ambient). Inlet circumferential velocity of the leakage flow could be varied by employing different inlet guide vanes. Further measurements have been carried out with higher rotor speeds and different labyrinth geometry, but no data has been available until now. Fig. 5 through 10 show some of the results taken from [7], together with the theoretical results obtained by the theory presented above. Agreement of both cross-coupling and damping coefficients with theory for both teeth on rotor and teeth on stator is more than satisfactory, keeping in mind that a stated experimental uncertainty of 7 kN/m for stiffness and 87.5 Ns/m for damping exists. Moreover inlet swirl velocity has not been measured directly but is calculated by knowing the guide outlet vane corrected by a factor obtained by guide vane cascade tests. No uncertainty is given here. Also the tested chamber geometry was not exactly modeled in the theory, theoretical results correspond to a tooth wall angle of 15° compared to 6° for the tested labyrinth. Nevertheless, the agreement is reasonably good, especially for the lower pressure ratios for non-choked flow conditions, which are the more realistic ones in practice. In the case of direct stiffness the theory gives a completely different dependence on inlet swirl as compared to the measurements. The measured coefficients change almost linearly with inlet swirl velocity, whereas theory gives a parabolic dependence and virtually zero stiffness without swirl. The experimental results are somewhat in contrast to other measurements, namely those by Benckert, where dependence on swirl is similar to that given by theory. This point has to be investigated further, since the influence of negative labyrinth stiffness on critical speeds and stability may be substantial, especially for back-to-back compressors with the piston labyrinth midspan. Most of the cross-coupled damping measurements are in the order of the given uncertainty. Theory here gives considerably larger values, at least for high inlet swirl. Moreover, the dependence on swirl as given by theory is linear whereas the measurements show little variation.

THE INTRINSIC IDENTITIES OF STATIC AND DYNAMIC COEFFICIENTS

The following simple kinematic reflections show that cross-coupling and direct damping forces are basically two different representations of the same physical phenomena. This is not further surprising, since they both have their origin in the fluid dissipation forces. We will further show that if the cross-coupling forces (as functions of inlet swirl velocity) are known, the damping forces can directly be determined from them. The same holds true for direct stiffness and cross-coupling damping. This implies then, that if the static forces (i.e. direct stiffness and cross-coupling) are known (for instance by measurements) for a sufficient range of inlet swirl velocities and with a sufficient accuracy, the dynamic forces (i.e. direct and cross-coupling damping) can be determined without further measurements. The above holds true if no centrifugal effects are present, which is generally tacitly assumed (otherwise, forces on the rotor would be different from those acting on the stator).

Let us consider a labyrinth with strips on the rotor (without loss of generality). The rotor has rotational speed Ω , eccentricity e and a velocity of the rotor center of Ωe , i.e. the rotor is rotating around the seal center. Let the inlet swirl velocity be w_{in} (see Fig. 11a). Then the lateral force F acting on the rotor is given by

$$F = (k_{Qrot} - b_{Rrot}\Omega)e,$$

where k_{Qrot} is the cross-coupling stiffness and b_{Rrot} the direct damping coefficient. Seen from the rotating reference frame (x',y'), the rotor is stationary, the stator rotates with $-\Omega$ and the inlet swirl velocity is $-(w_{rot}-w_{in})$, where w_{rot} is the circumferential rotor speed (see Fig. 11b). With the above assumption i.e no centrifugal effects, the forces have not changed by the change of coordinates and by the same token we can interchange rotor and stator without changing the forces (Fig. 11c), i.e. we have now a seal with teeth on stator, static eccentricity e , rotor speed $-\Omega$ and inlet swirl velocity $-(w_{rot}-w_{in})$. The force acting on the rotor is now simply a cross-coupling force $k_{Qstat}e$ in the opposite direction of F . Setting the two forces equal, we obtain the following equation:

$$k_{Qrot}(w_{in}) - b_{Rrot}(w_{in})\Omega = -k_{Qstat}(w_{rot}-w_{in}),$$

or

$$b_{Rrot}(w_{in}) = 1/\Omega [k_{Qrot}(w_{in}) + k_{Qstat}(w_{rot}-w_{in})]. \quad (11)$$

Hence, the damping coefficient is completely determined by cross-coupling coefficients. For stiffness and cross-coupling damping the same reasoning leads to

$$b_{Qrot}(w_{in}) = 1/\Omega [k_{Rstat}(w_{rot}-w_{in}) - k_{Rrot}(w_{in})]. \quad (12)$$

Since both expressions involve differences, the practical value for determining damping coefficients may be questionable. However, the identities may be used for either a check for measurement accuracy or for secondary effects not included in the theory. Also it follows from the identities that a theory which predicts well cross-coupling stiffness will also predict damping with the same accuracy and the same is true for the other two coefficients. Therefore, it is no coincidence that the presented theory performs equally well for cross-coupling and damping.

WATER OPERATED TEST STAND FOR ROTORDYNAMIC FORCE MEASUREMENTS

A test rig has been set up at the Institut für Flüssigkeitstechnik at the Federal Institute of Technology in Zurich, Switzerland. It is water operated and was initially designed for the measurements of rotor-dynamic coefficients of hydraulic seals for pumps and water turbines. Important features of this test rig are the high measuring accuracy, which allows precise measurements even at zero inlet swirl and low rotor speeds, the separate measurement of the individual chambers and the hydraulically operated stator, allowing various orbit configurations, such as circular orbits. Rotor speed varies between 0 and 3570 RPM (i.e. 0 - 67 m/s), pressure up to 8 bar, stator frequency up to 30 Hz. Inlet swirl is either zero or close to rotor circumferential speed (produced by rotor blades). The pressure distribution is measured in the individual chambers by static and dynamic pressure probes, inlet swirl velocity by total pressure probes. Fig. 12 gives a cross section of the test stand and Fig.13 a schematic of the hydraulic stator drive. Fig. 14 shows the test stand after installation (Figures by courtesy of Institut für Flüssigkeitstechnik, Federal Institute of Technology, Zurich Switzerland). Up to now, only static measurements of direct stiffness and cross-coupling stiffness have been carried out with no inlet swirl. The first measurements have been carried out with a three chamber straight-through labyrinth seal with teeth on the stator. Fig. 15 shows the results of the measurements of the different chambers for different pressures and rotor speeds. An interesting fact is the positive stiffness in the first chamber. It may be explained by the circumferential variation of the axial friction losses in an eccentric seal (also called Lomakin effect [4], [5]). For a plain annular seal the centering stiffness coefficient is given by ([9]):

$$k = \Delta p \frac{rl^2}{2\Delta r^2(\lambda l/2\Delta r + 1)^2} \pi \lambda^4 e,$$

where Δp is the pressure drop along the seal, l the length, Δr the radial clearance and λ the pipe flow number. Considering the first labyrinth chamber as a plain annular seal with clearance equal to tip clearance, we obtain the values for k very close to the measured direct stiffness (see Fig. 16), at least for the lower rotor speeds. Hence it seems that for direct stiffness the first chamber acts rather like a plain annular seal. Even in the second and third chamber the direct stiffness shows anomalous behaviour for the lower rotor speeds, only for high rotor speed is the behaviour as predicted by theory, i.e. a reduction of the (negative) stiffness with increasing pressure difference. This reduction is a consequence of the smaller pick-up of circumferential speed in the chambers with the increase of axial flow with pressure difference. For gas seals, where the density increases with pressure, the (negative) stiffness increases also (see Fig. 7 and 8). Another interesting feature is the strong dependence of the stiffness on rotor speed as predicted by theory. This is in contrast to the measurements by Scharer [7], where stiffness was virtually independent of rotor speed. Cross-coupling stiffness shows an expected negative sign, but it increases from first to second chamber as opposed to theory. Again, it seems that the first chamber is behaving differently compared to the following ones. As in the comparison for the short labyrinth in Fig. 4 for zero inlet swirl, the theory gives generally larger cross-coupling stiffness (in the algebraic sense) compared to measurement. Since the cross-coupling forces are very small at zero swirl compared to practical inlet swirl velocities found in reality (without swirl brakes), this does not impair seriously the theory for predicting rotor stability, as long as damping coefficients are predicted accurately. Further measurements will include damping coefficients with circular or elliptical orbits of the stator and measurements with inlet swirl velocity.

CONCLUSIONS

The theoretical prediction of cross-coupling and damping coefficients has been corroborated by several independent measurements for different rotor speeds and inlet swirl velocities of the leakage flow, the most important ones being the gas seal tests at the Turbomachinery Laboratories at Texas A&M University. In particular, it has been shown that the damping coefficients of the seals are behaving as predicted by theory, i.e. they are insensitive to a wide range of inlet swirl velocities. This has important consequences for the design of high pressure centrifugal compressors, where the seals may be considered as passive dampers for rotor vibrations. For the direct stiffness and the cross-coupling damping coefficients, the theory differs largely from measurements, at least for the gas seal measurements from Texas A&M University. Here, further work is necessary on the theoretical and also on the experimental side. The water operated test stand presented gives new insights into the behaviour of labyrinth seals due to its high measuring resolution and the possibility of measuring individual chambers. Further measurements may show the way how to resolve the discrepancy between theory and measurements for direct stiffness and cross-coupling damping.

REFERENCES

1. Abramovich, G. N., *The Theory of Turbulent Jets*, MIT Press, Cambridge, Mass., 1963.
2. Benckert, H., ""Spaltströmung." Forschungsberichte Forschungs- vereinigung Verbrennungskraftmaschinen," Frankfurt, Vol. 252, 1978.
3. Childs, D. W., and Scharrer, J. K., "Experimental Rotordynamic Coefficient Results for Teeth-on-Rotor and Teeth-on-Stator Labyrinth Gas Seals," Mechanical Engineering Department, Turbomachinery Laboratories, Texas A&M University, College Station, Texas 77843.
4. de Salis, J., "Lomakin-Effekt bei Durchblicklabyrinth ?," Interner Bericht 635-9, Institut für Flüssigkeitstechnik, Eidg. Techn. Hochschule, Zürich, 1984.
5. Lomakin, A. A., "Die Berechnung der kritischen Drehzahl und der Bedingungen für dynamische Stabilität der Läufer von Hochdruckströmungs- maschinen unter Berücksichtigung der in der Dichtung auftretenden Kräfte (in Russian)," *Energomasinostroenie*, Vol. 4, 1958, pp. 1-5.
6. Neumann, K., "Zur Frage der Verwendung von Durchblickdichtungen im Dampfturbinenbau," *Maschinentechnik*, Vol. 13, 1964, Nr.4
7. Scharrer, J. K., "A Comparison of Experimental and Theoretical Results for Rotordynamic Coefficients for Labyrinth Gas Seals," Turbomachinery Laboratories Report No. SEAL-2-85, Texas A&M University, May 1985.
8. Stoff, H., "Calcul et mesure de la turbulence d'un écoulement incompressible dans le labyrinthe entre une arbre en rotation et un cylindre stationnaire," Thesis No. 342 (1979) Swiss Federal Institute of Technology, Lausanne, Juris Verlag Zürich, 1979.
9. Trutnovsky, K., *Berührungsfreie Dichtungen*, VDI Verlag, 1973.
10. Wyssmann, H., Pham, T. C. and Jenny, R., "Prediction of Stiffness and Damping Coefficients for Centrifugal Compressor Labyrinth Seals," *Journal of Engineering for Gas Turbines and Power*, Vol. 106, 1984, pp. 920-926.

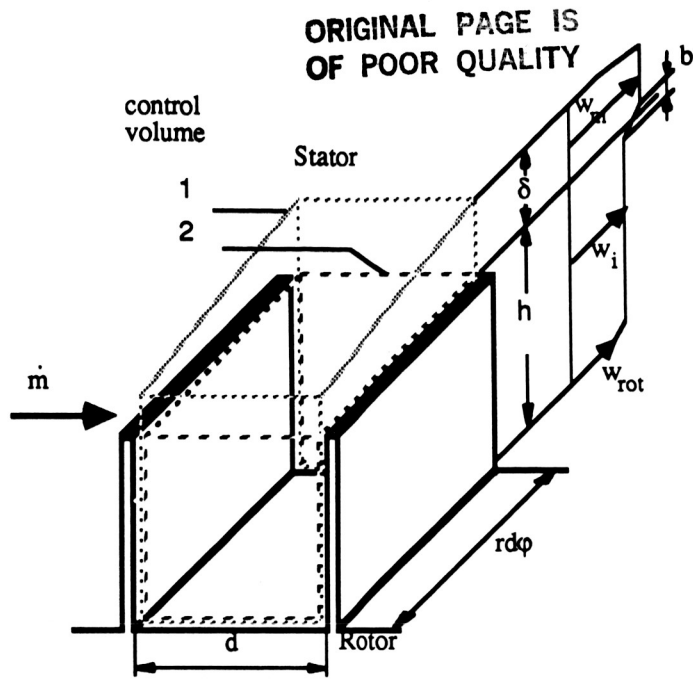


Fig. 1 Control volumes and circumferential velocity of the straight labyrinth

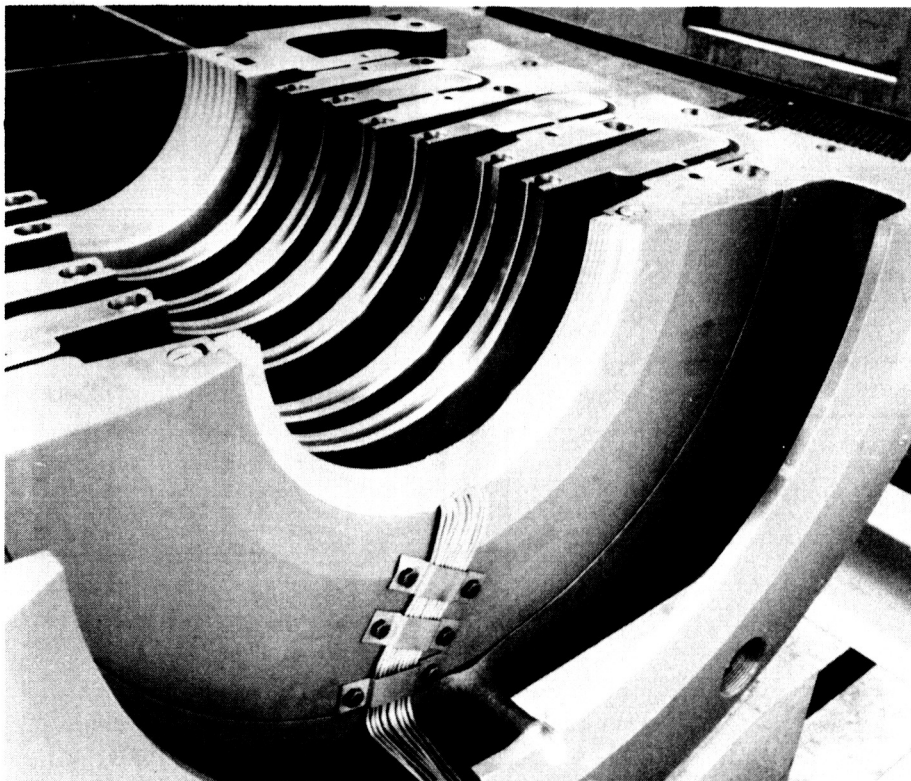


Fig. 2 Test labyrinth in the casing bottom half

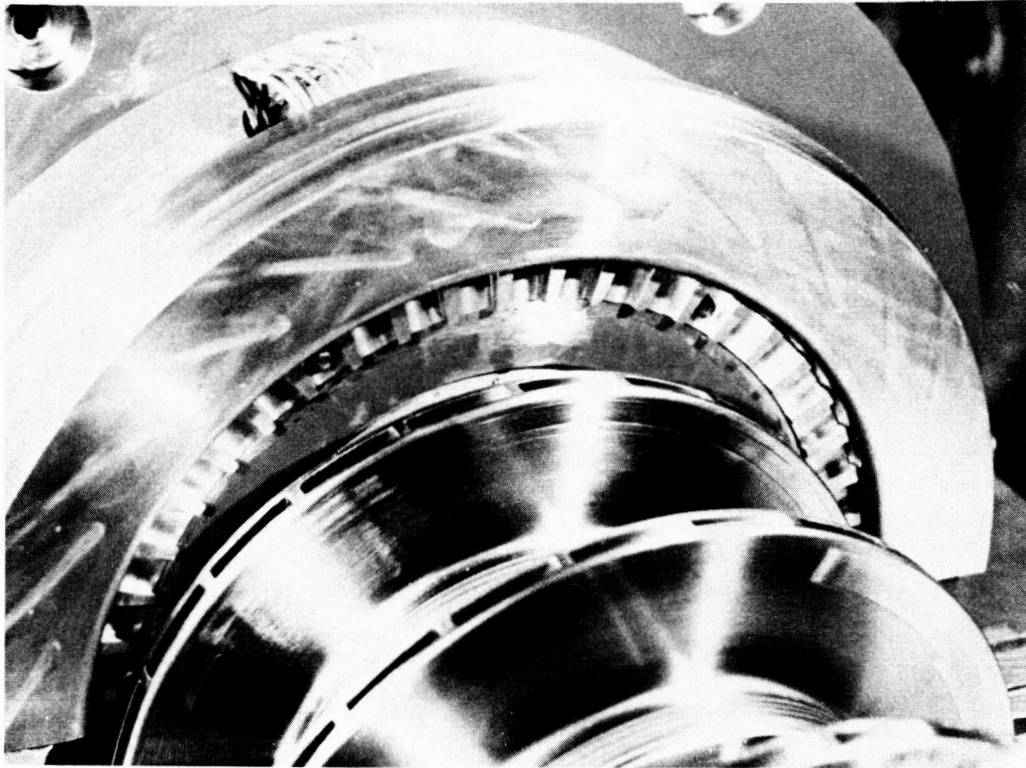


Fig. 3 Swirl brake installed in high pressure centrifugal compressor

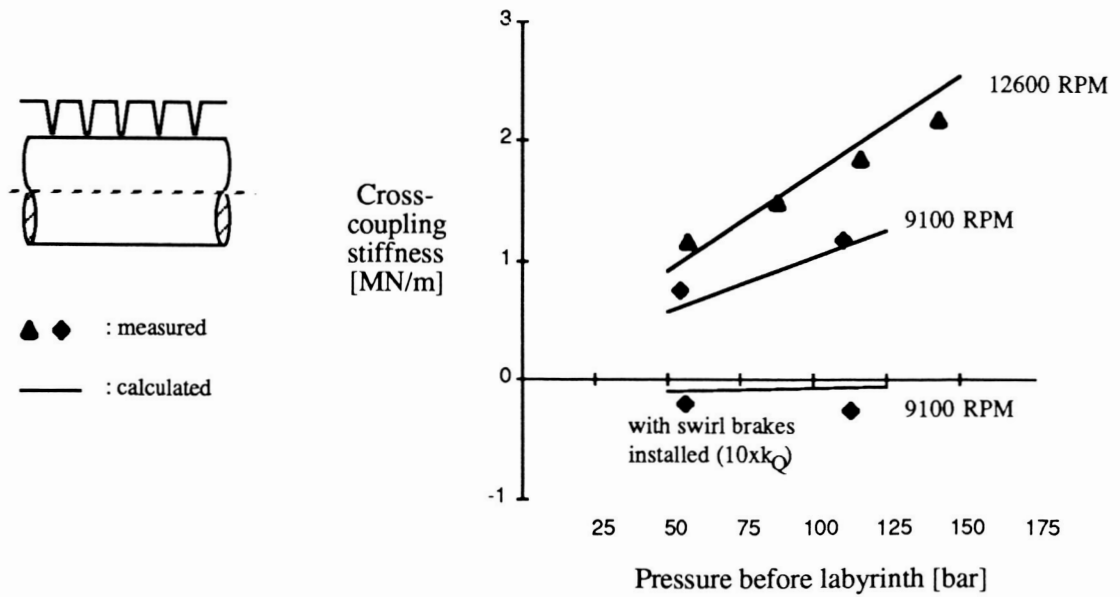
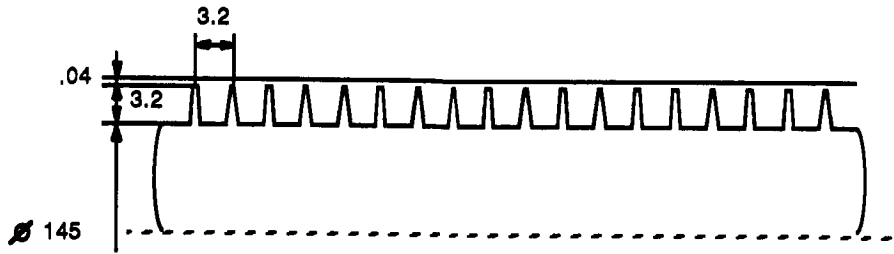


Fig. 4 Measurement vs. theory for cross-coupling coefficients of high pressure centrifugal compressor



Rotor Speed: 3000 RPM
Pressure Ratio: 3.08

▲ : measured
△ : calculated

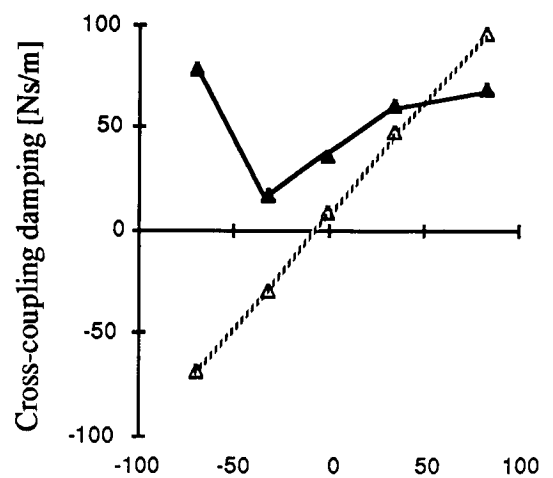
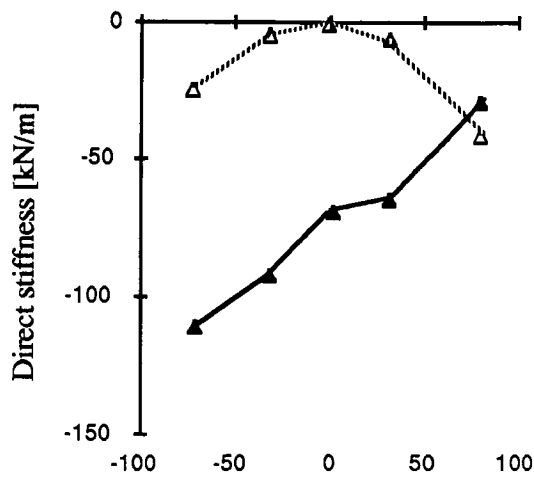
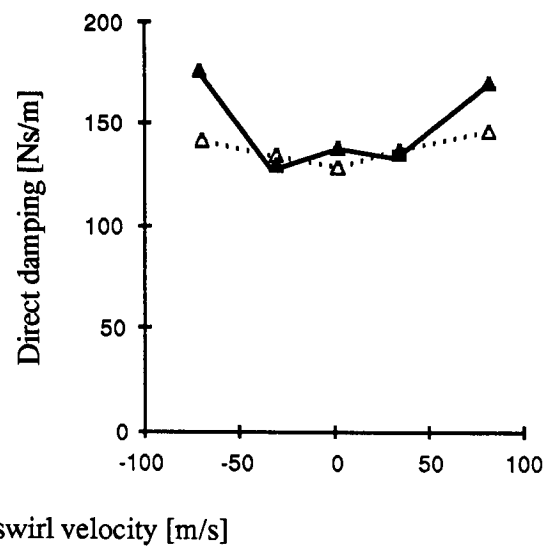
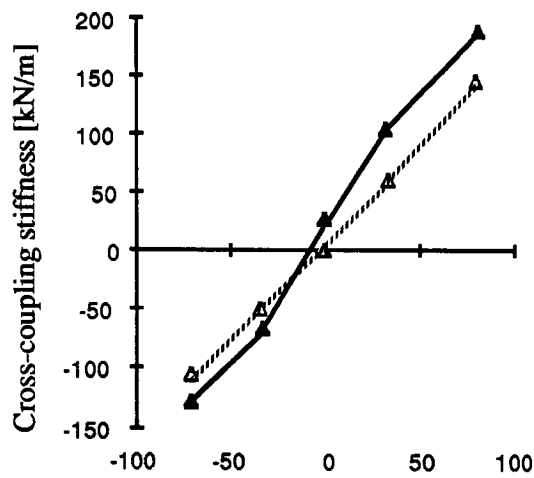
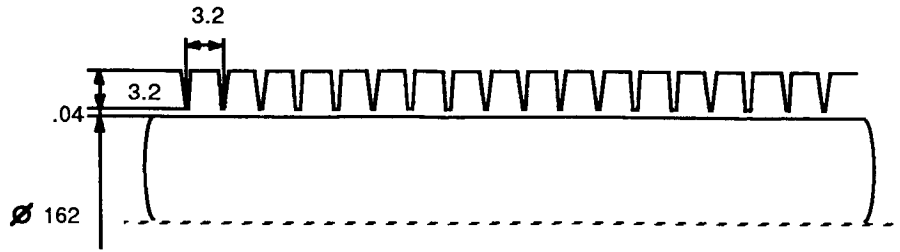
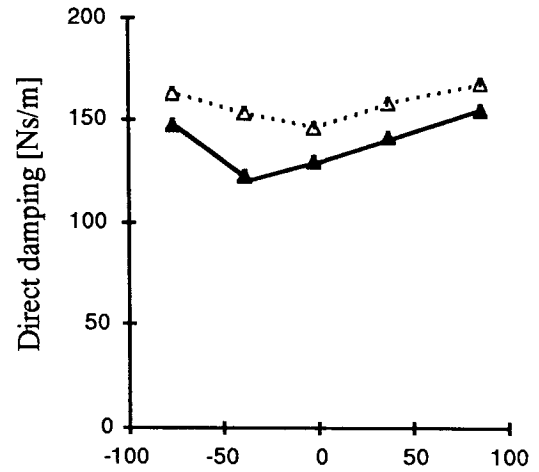
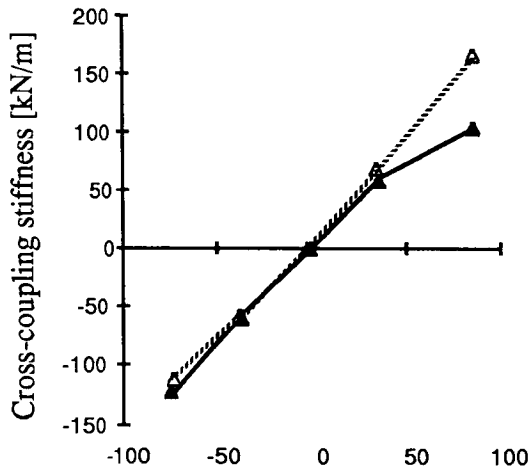


Fig. 5 Labyrinth coefficients vs. inlet swirl velocity for teeth on rotor labyrinth (measurements from [7])

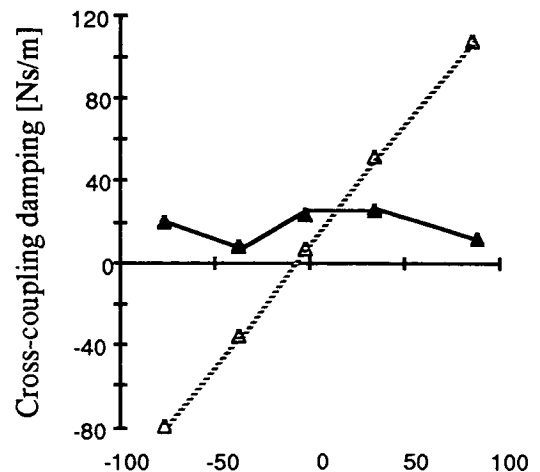
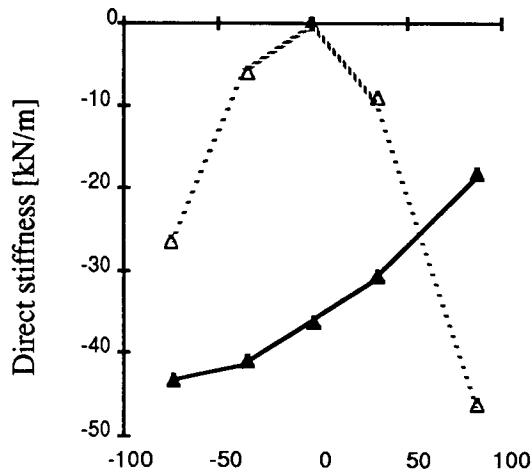


Rotor Speed: 3000 RPM
Pressure Ratio: 3.08

▲ : measured
△ : calculated

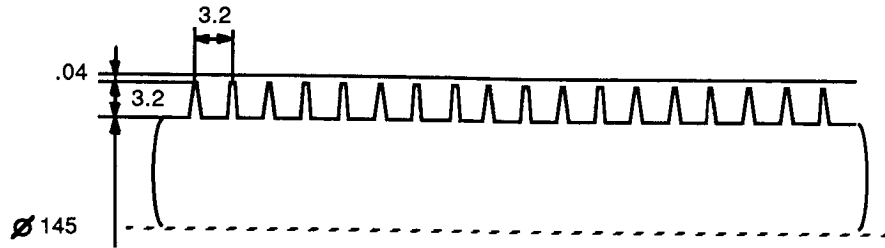


Inlet swirl velocity [m/s]



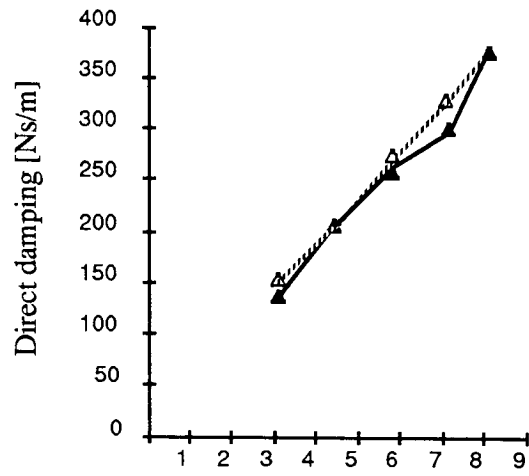
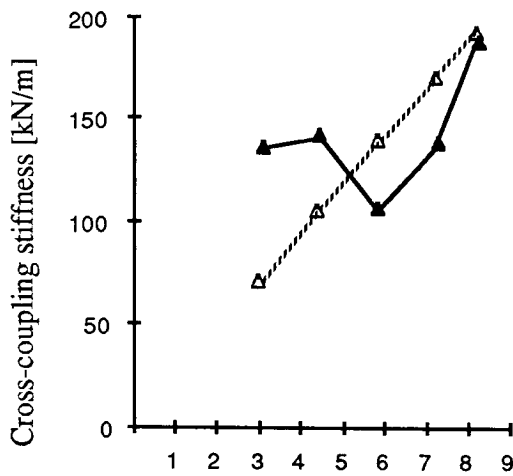
Inlet swirl velocity [m/s]

Fig. 6 Labyrinth coefficients vs. inlet swirl velocity for teeth on stator labyrinth (measurements from [7])

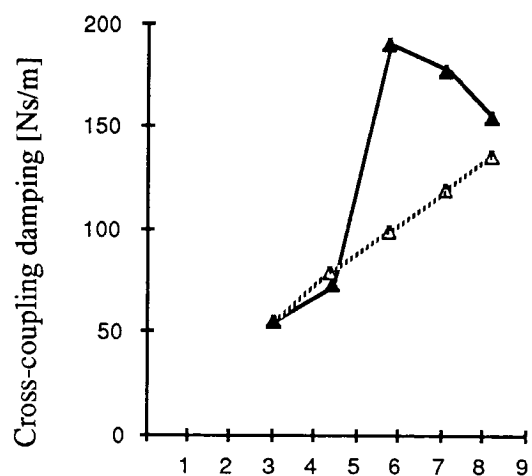
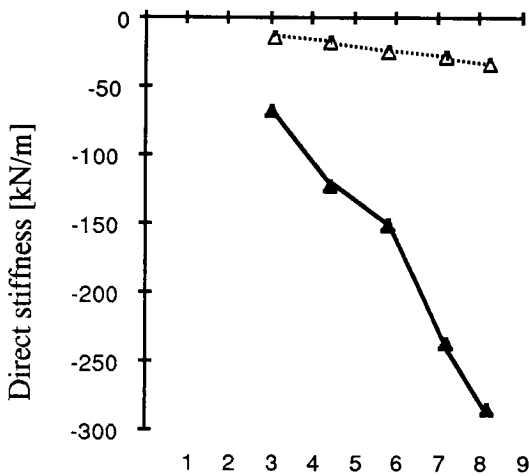


Rotor speed: 8000 RPM
 Inlet swirl velocity: 37 m/s

▲ : measured
 △ : calculated

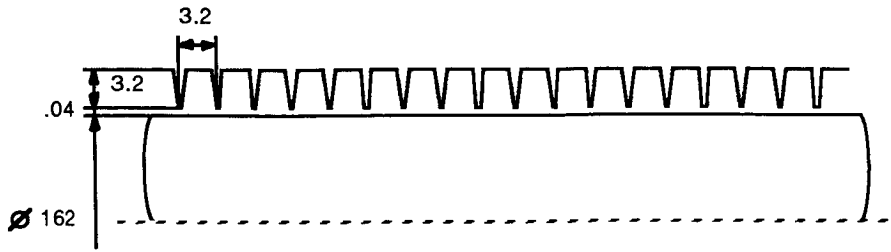


Pressure ratio



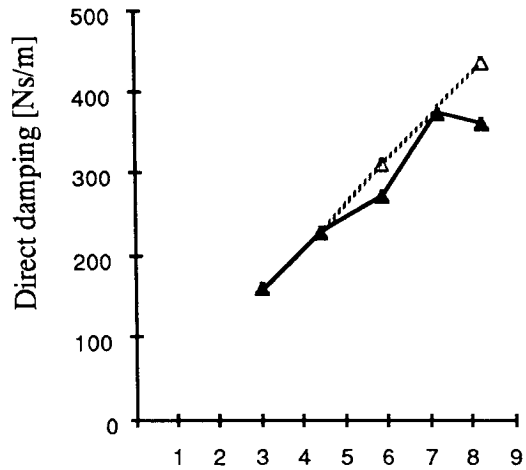
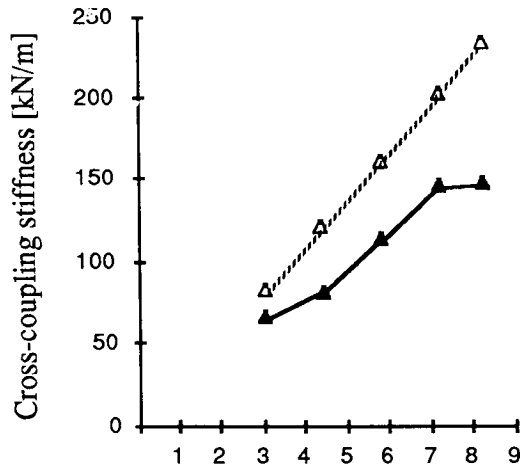
Pressure ratio

Fig. 7 Labyrinth coefficients vs. pressure ratio for teeth on rotor labyrinth (measurements from [7])

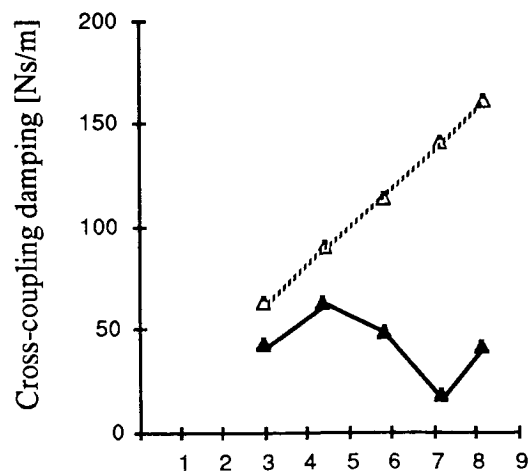
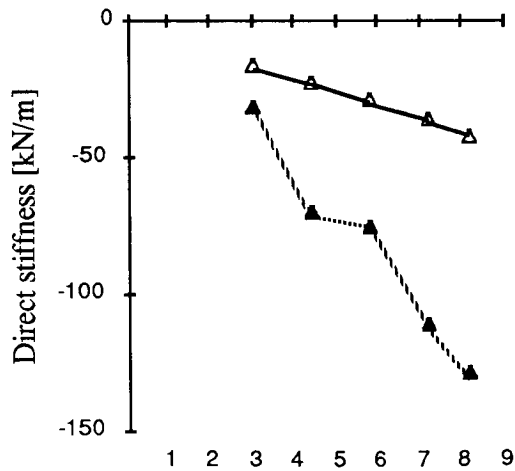


Rotor speed: 8000 RPM
Inlet swirl velocity: 41 m/s

▲ : measured
△ : calculated

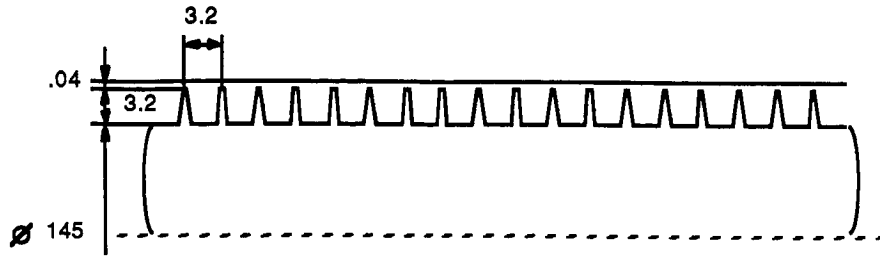


Pressure ratio



Pressure ratio

Fig. 8 Labyrinth coefficients vs. pressure ratio for teeth on stator labyrinth (measurements from [7])



Pressure ratio: 3.08
 Inlet swirl velocity: 36 m/s

▲ : measured
 △ : calculated

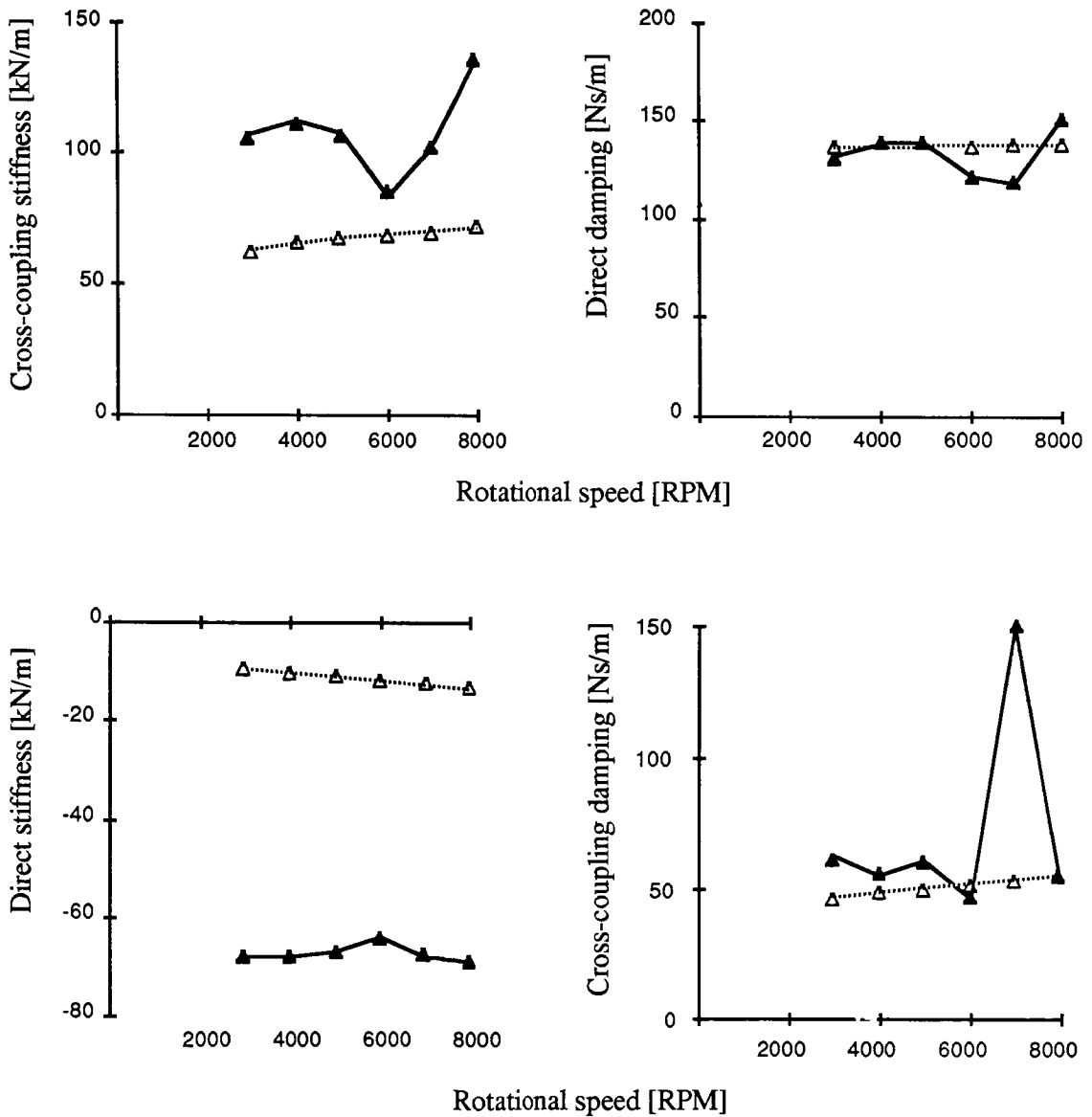
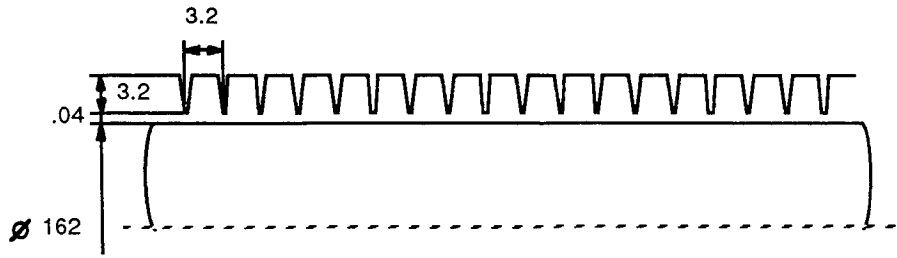


Fig. 9 Labyrinth coefficients vs. rotor speed for teeth on rotor labyrinth (measurements from [7])



Pressure ratio: 3.08
 Inlet swirl velocity: 41 m/s

▲ : measured
 △ : calculated

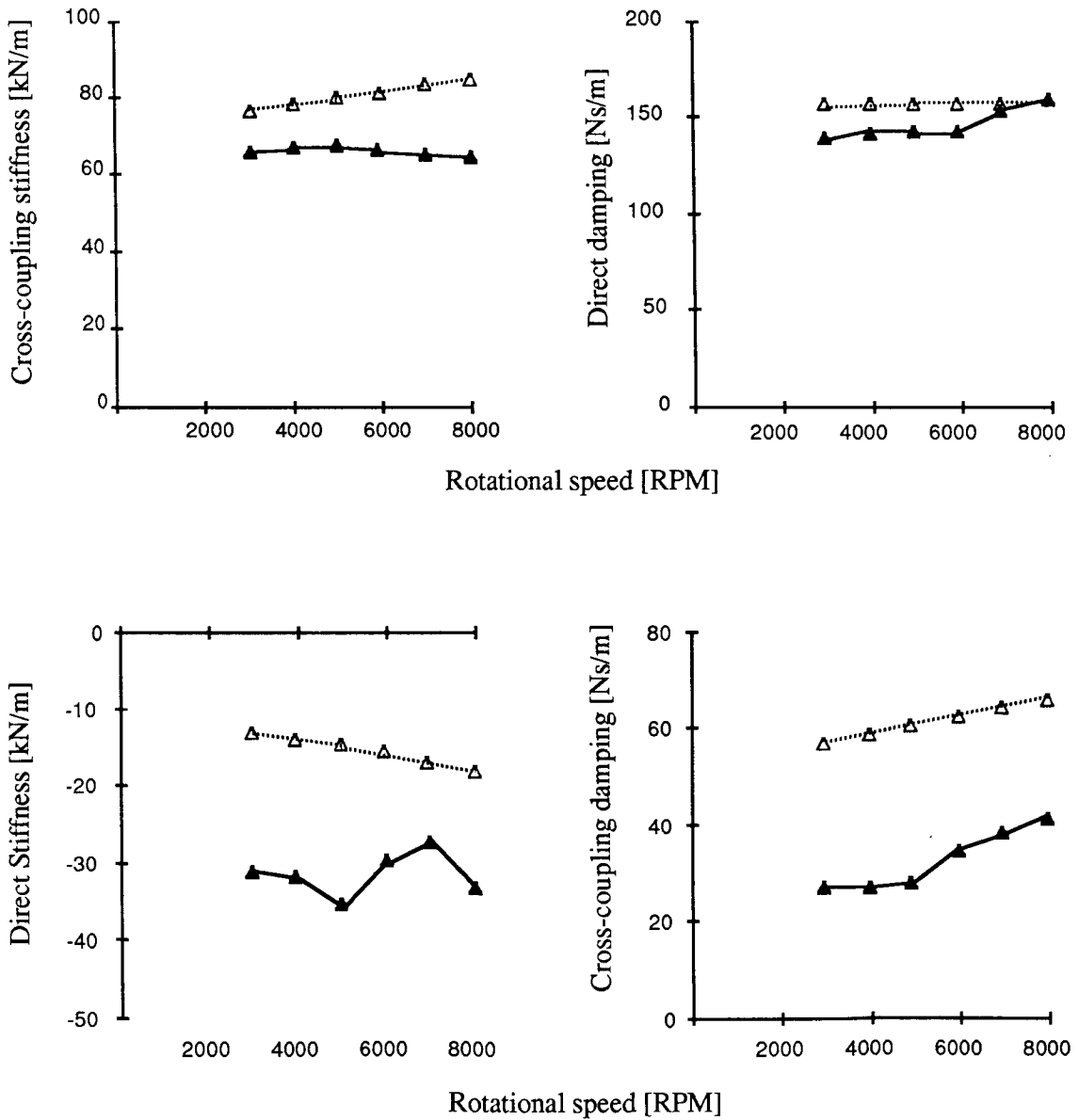


Fig. 10 Labyrinth coefficients vs. rotor speed for teeth on stator labyrinth (measurements from [7])

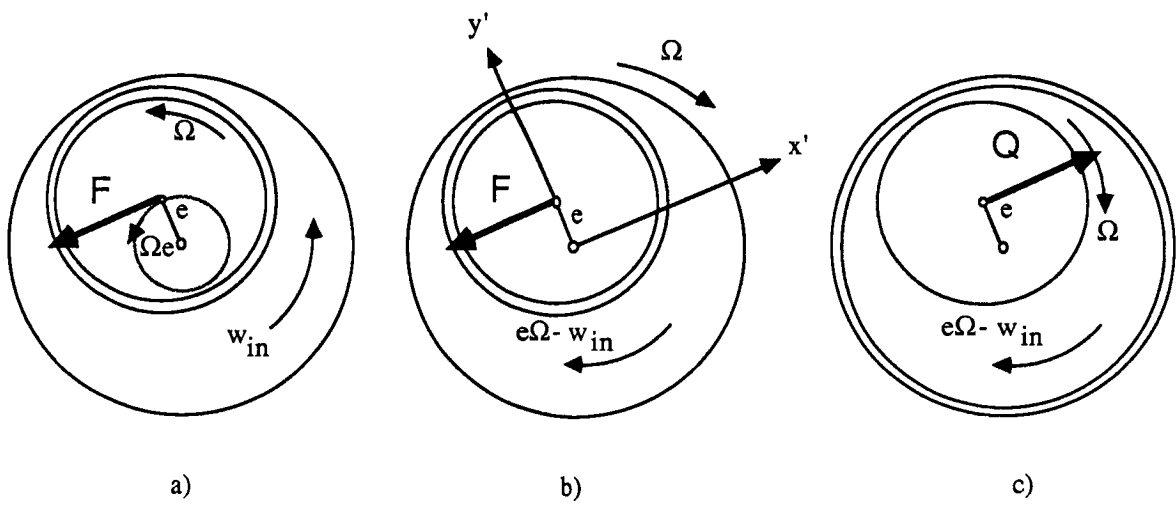


Fig. 11 The basic identity of cross-coupling and damping forces

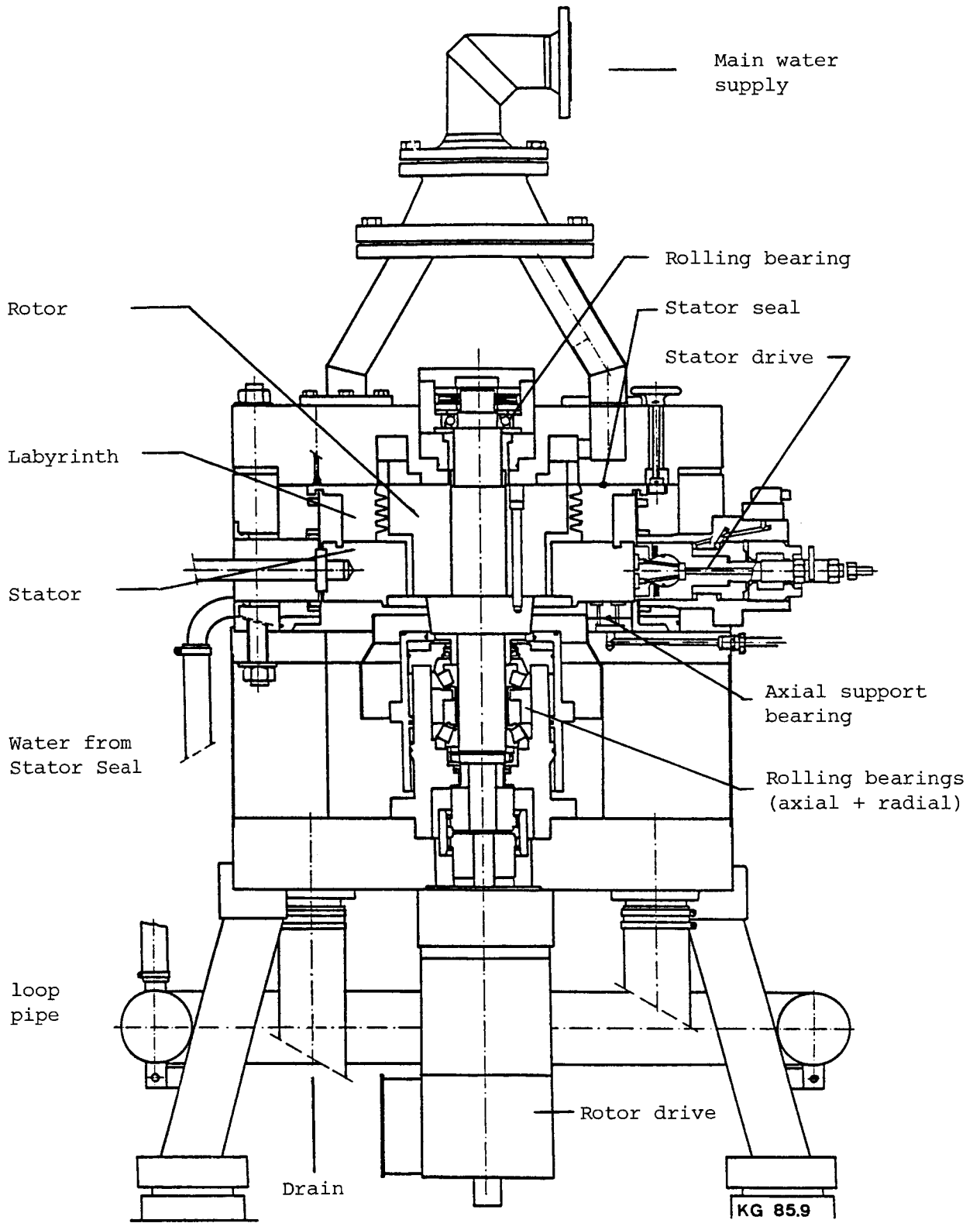


Fig. 12 Cross-section of water operated labyrinth test stand

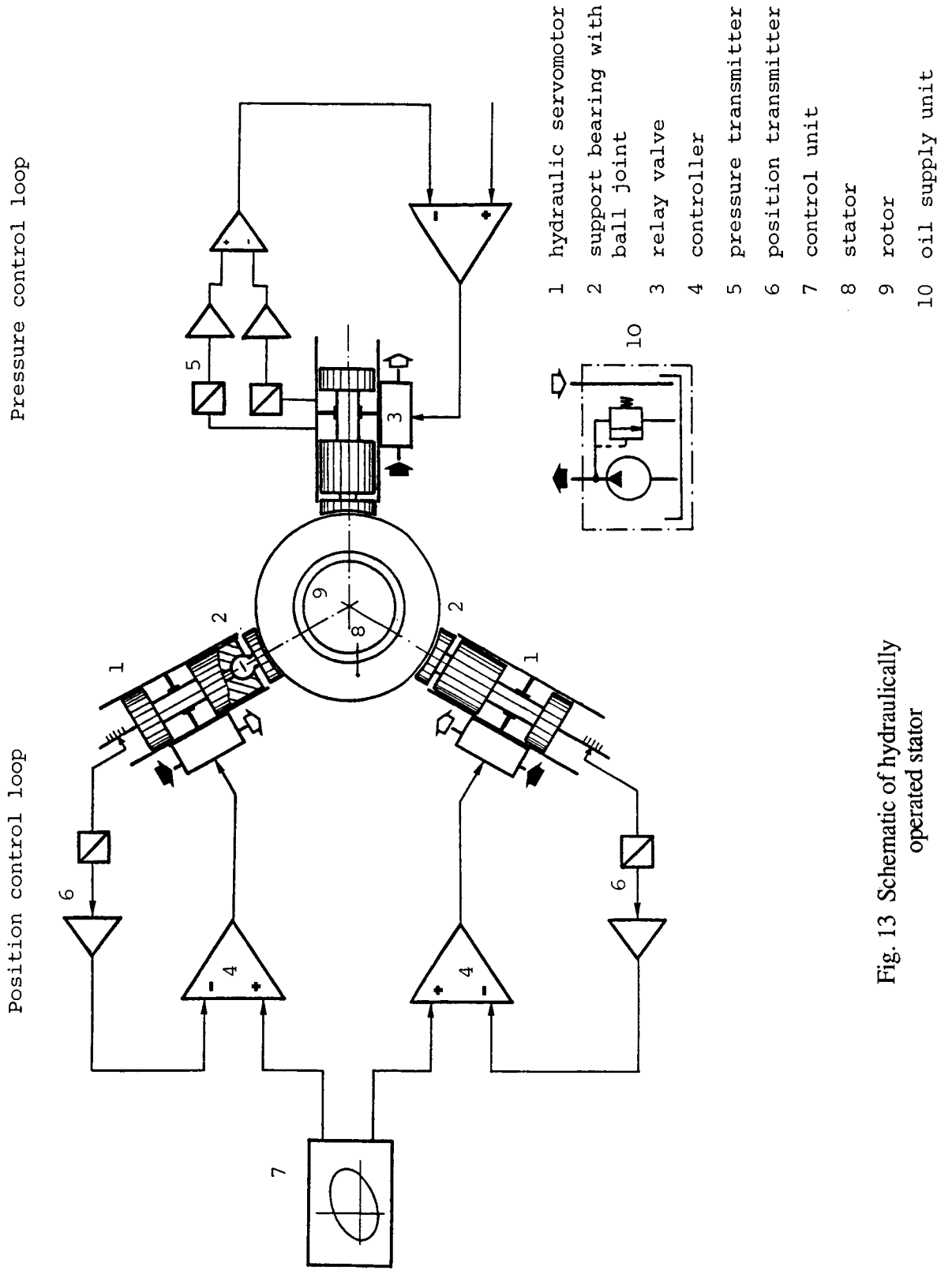


Fig. 13 Schematic of hydraulically operated stator

ORIGINAL PAGE IS
OF POOR QUALITY

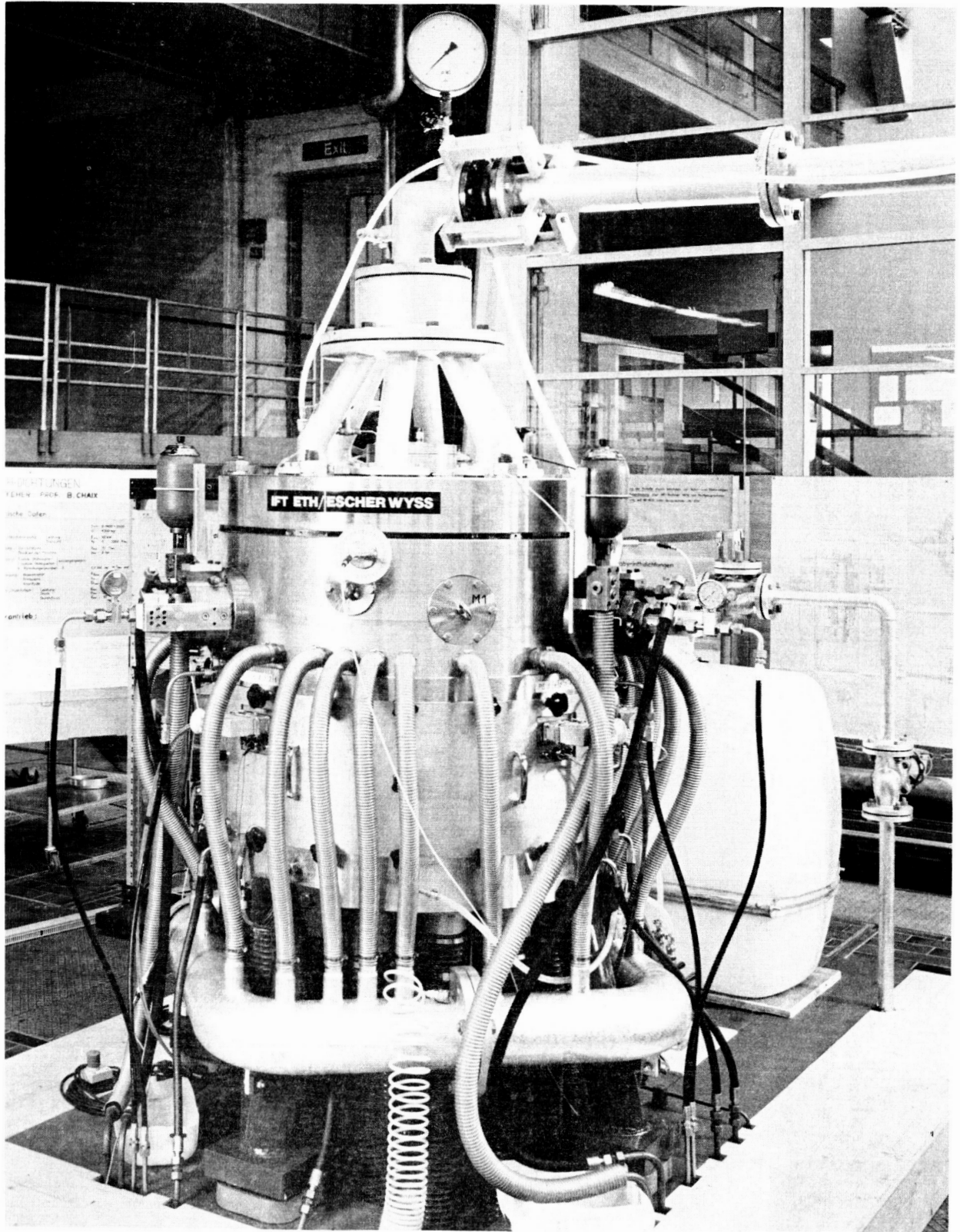


Fig. 14 Water operated labyrinth test stand

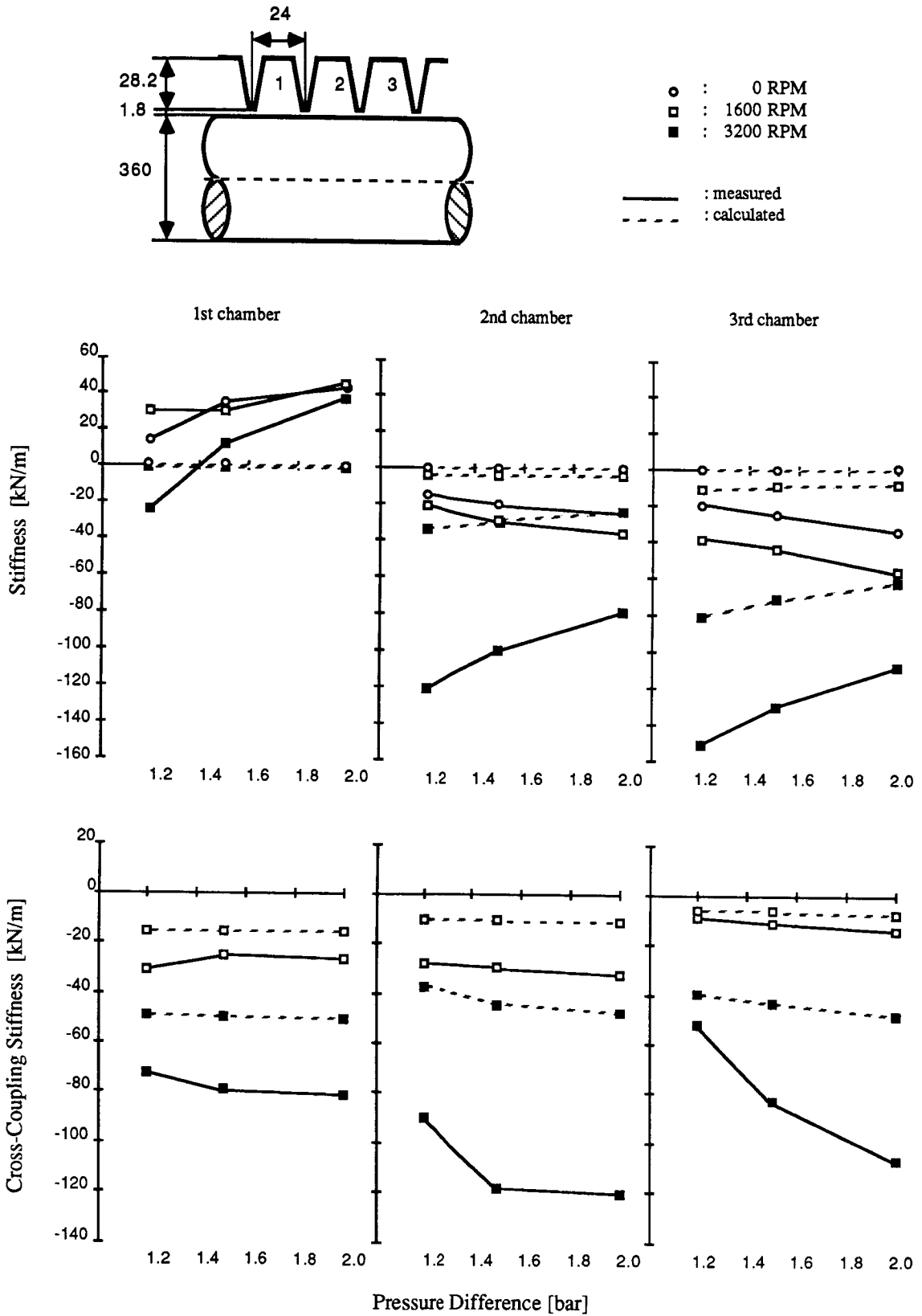


Fig. 15: Measurement of stiffness and cross-coupling stiffness without inlet swirl (water tests)

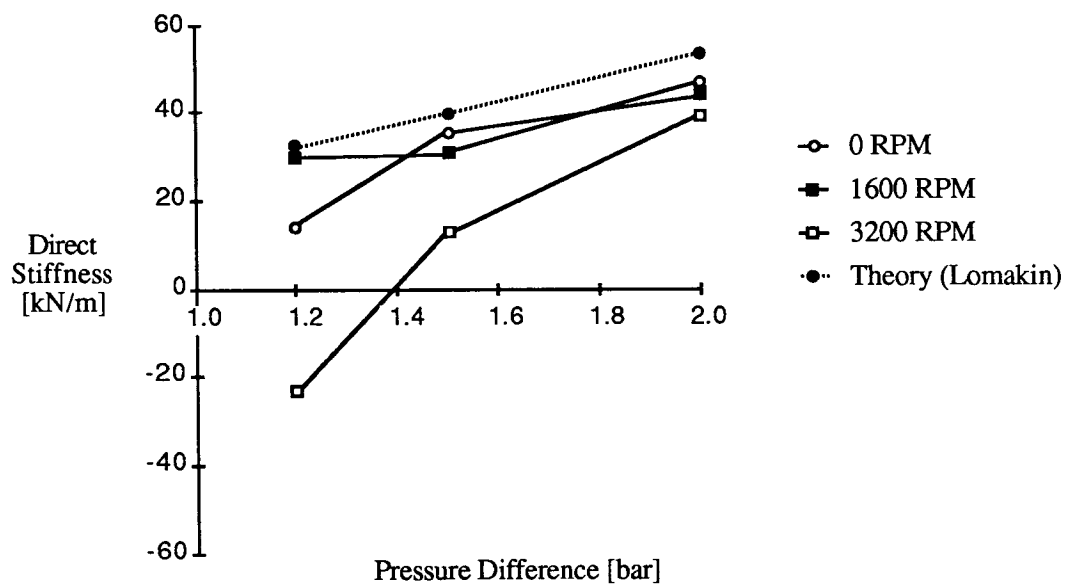


Fig. 16 Comparison with Lomakin formula